Secondary gigantic jets as possible inducers of sprites

Li-Jou Lee,[1] Rue-Ron Hsu,[1] Han-Tzong Su,[1] Sung-Ming Huang,[1] Jung-Kung Chou,[1] Cheng-Ling Kuo,[2] Shu-Chun Chang,[1] Yen-Jung Wu,[1] Alfred B. Chen,[3] Harald U. Frey,[4] Yukihiro Takahashi,[5] and Lou-Chuang Lee[2,6]

Received 27 January 2013; revised 26 February 2013; accepted 26 February 2013; published 25 April 2013.

[1] Three multi-transient luminous events, which were recorded by ISUAL on FORMOSAT-2 and shared a similar generating sequence, are reported. Each event began with a positive cloud-to-ground lightning discharge (CG)-induced sprite, and a secondary gigantic jet (GJ) followed within ~30–50 ms. Then, 1 ms after the GJ, a new sprite occurred near the GJ without associated impulsive lightning signal. The associated electromagnetic signal for one of the events indicates that the GJ is a negative cloud-to-ionosphere discharge carrying a high peak current moment. Cross-analysis of the spectral, image, and electromagnetic data of these three events indicates that the new sprites are likely induced by the secondary GJs, and the high current moment of the secondary GJs appears to be a crucial factor for the induction of the new sprites. Hence, these secondary GJs may have played a role in inducing sprites as much as the negative CGs do for the occurrence of negative sprites.
Citation: Lee, L.-J., R.-R. Hsu, H.-T. Su, S.-M. Huang, J.-K. Chou, C.-L. Kuo, S.-C. Chang, Y.-J. Wu, A. B. Chen, H. U. Frey, Y. Takahashi, and L.-C. Lee (2013), Secondary gigantic jets as possible inducers of sprites, *Geophys. Res. Lett.*, *40*, 1462–1467, doi:10.1002/grl.50300.

1. Introduction

[2] Sprites and gigantic jets (GJs) are both members of the transient luminous events (TLEs), while their generating mechanisms and morphologies differ. Sprites are fleeting luminous emissions spanning the altitudes of ~40–90 km above active thunderstorms [*Sentman et al*., 1995] and are usually induced by the quasi-electrostatic field established by positive cloud-to-ground lightning discharges (+CGs) [*Pasko et al*., 1997]. However, though only very rarely, sprites have also been documented to be triggered by negative CGs (−CGs) [*Barrington-Leigh et al*., 1999; *Taylor et al*., 2008; *Li et al*., 2012]. On the other hand, gigantic jets are upward propagating discharges that bridge the thundercloud top and the ionosphere [*Pasko et al*., 2002; *Su et al*., 2003; *van der Velde et al*., 2007; *Cummer et al*., 2009; *Kuo et al*., 2009; *Chou et al*., 2010; *van der Velde et al*., 2010; *Lu et al*., 2011; *Huang et al*., 2012] and can be considered as upward discharging counterparts of cloud-to-ground lightning discharges [*Krehbiel et al*., 2008]. Therefore, it is natural to ponder whether GJs are also capable of inducing sprites.

[3] Complex TLEs, which contain both sprites and jets, had previously been reported. For some of these events, the event sequence started with a sprite which then appeared to have affected the occurrence of closely following secondary jets [*Marshall and Inan*, 2007, and references therein] or secondary gigantic jets [*Lee et al*., 2012]. Interestingly, *van der Velde et al*. [2010] reported that in a complex TLE, a positive GJ with high current moment occurred first, followed by a sprite about 80 ms later, although the sprite was induced independently by a +CG.

[4] Between July 2004 and December 2010, the Imager of Sprites and Upper Atmospheric Lightning (ISUAL) on FORMOSAT-2 has also captured a few of these complex events amidst the 17,000 plus TLEs. Among them, event A (Figure 1; 9 December 2009 14:40:04 UTC; over northern Australia), event B (not shown; 3 August 2006 23:33:43 UTC; over West Africa), and event C ([*Lee et al*., 2012, Figure 1d]; 30 September 2008 21:52:44 UTC; over central Africa) have similar evolution sequences and are particularly interesting. The event sequence always began with a +CG-induced sprite which was then followed by a secondary GJ ~30–50 ms later. Meanwhile, about 1 ms right after the occurrence of the GJ, a new sprite appeared near the fringing region of the GJ. In this article, optical, spectral, and electromagnetic data are presented that support the concept of the new sprites likely being induced by the secondary GJs. The possible physical conditions for the secondary GJs to induce sprites are also deduced and discussed.

2. Instruments and Data

[5] The data analyzed in this paper are from the ISUAL experiment and the National Cheng Kung University (NCKU) sferics recording station. ISUAL is the scientific payload onboard the FORMOSAT-2 satellite, which moves along a Sun-synchronized orbit at 891 km altitude. ISUAL is configured with an eastward limb view, to detect TLEs and lightning in the night hemisphere [*Chern et al*., 2003; *Chen et al*., 2008; *Lee et al*., 2010]. The ISUAL payload consists of three main sensors: an intensified CCD imager (Imager), a six-channel spectrophotometer (SP), and a dual-module array photometer (AP). The imaging area of the ISUAL CCD is 512 pixels × 128 pixels, with a field-of-view (FOV) of 20°(H) × 5°(V). Generally, ISUAL records six

[1]Department of Physics, National Cheng Kung University, Tainan, Taiwan.
[2]Institute of Space Science, National Central University, Jhongli, Taiwan.
[3]Institute of Space, Astrophysical and Plasma Sciences, National Cheng Kung University, Tainan, Taiwan.
[4]Space Sciences Laboratory, University of California, Berkeley, California, USA.
[5]Department of Cosmosciences, Hokkaido University, Sapporo, Japan.
[6]Institute of Earth Sciences, Academia Sinica, Taipei, Taiwan.

Corresponding author: R.-R. Hsu and H.-T. Su, Department of Physics, National Cheng Kung University, Tainan, Taiwan. (rrhsu@phys.ncku.edu.tw); (htsu.@phys.ncku.edu.tw)

0094-8276/13/10.1002/grl.50300

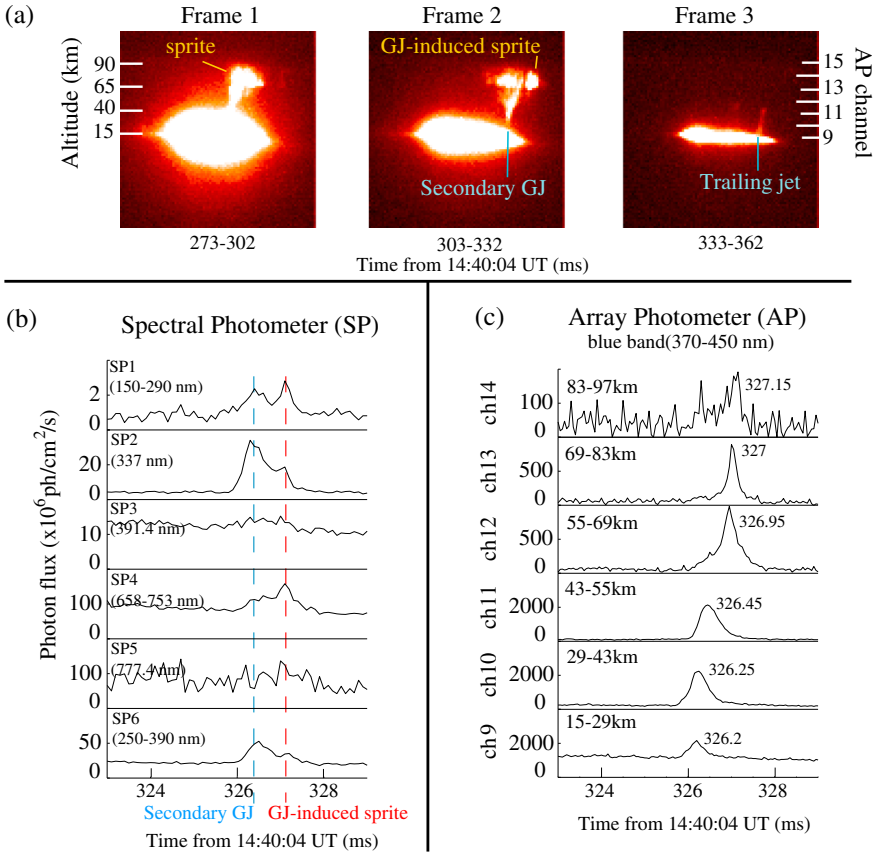

Figure 1. Cropped image sequence and photometric signals for event A. (a) The cropped images were recorded by the ISUAL imager through a $N_2$1P (623–750 nm) filter, with the frame integration time of 29 ms and a 1 ms dead time between frames. (b) The corresponding spectrophotometer data for the interval of 323–329 ms (relative to 14:40:04.000 UTC), which contain emissions from the GJ and the GJ-induced sprite. (c) The array photometer blue module data for the interval 323–329 ms; only the channels covering the altitudes of the GJ and the sprites are shown.

consecutive image frames for each event trigger, with a frame integration time of 29 ms and a 1 ms dead time between frames.

[6] The SP shares the same bore-sighted FOV with the imager. The time resolution for the SP data is 0.1 ms. For each event trigger, the data range of the SP data is from 24 ms before the trigger to 181 ms after. The SP contains six independent channels: SP1 (150–290 nm; FUV, N_2 LBH band), SP2 (335–341.2 nm, centered at 337 nm; $2PN_2(0,0)$), SP3 (387.1–393.6 nm, centered at 391 nm; $1NN_2^+(0,0)$), SP4 (658.9–753.4 nm; $1PN_2$), SP5 (centered at 777.4 nm; O_I emission in lightning), and SP6 (250–390 nm; MUV, $2PN_2$). The ISUAL AP contains two modules; each comprises 16 vertically stacked anode photometers with the blue module covering the 370–450 nm wavelength band and the red module covering the 530–650 nm band. An AP channel has a FOV of 22°(H) × 0.23°(V), and an AP module has a combined FOV of 22°(H) × 3.6°(V). The AP sampling rate is 20 kHz from 8 ms before an event trigger to 20 ms after and drops down to 2 kHz until 240 ms after the trigger. The ISUAL AP provides temporal and spatial resolving photometric data.

[7] The NCKU magnetic ultralow frequency (ULF) station (0.3 to 500 Hz) is located at the Lulin observatory, which is on the central mountain ridge of Taiwan [*Huang et al.*, 2011]. The system consists of a pair of EMI-BF4 magnetic induction coils to record the horizontal magnetic field. The NCKU ULF station has been rebuilt several times after it was damaged by lightning and has only been operated continuously since June 2009. The recorded signals are used to infer the polarity, the vertical current moment, and the time-integrated charge moment change (CMC) of TLEs and lightning. The analyzing method can be found in the works of *Cummer* [2003], *Cummer et al.* [2009], and *Huang et al.* [2012].

3. Analysis of the ISUAL Data

3.1. Optical Data

[8] As shown in Frame 1 of Figure 1a, event A begins as a clustering sprite that is induced by a positive CG lightning (Figure 2b). About 40 ms later (in Frame 2), a secondary GJ develops through the center region of the previous sprite, along with a nearby new sprite. This new sprite is located near the fringing region of the clustering sprite and the secondary GJ, while they may have slightly overlapped. In Frame 3, only the trailing jet of the GJ remains visible. The exposure time of the image frames is 29 ms, and thus, the occurrence order of the GJ and the sprite in the second frame cannot be resolved from the image. It should be noted that for event C [see *Lee et al.*, 2012, Figure 1d], the secondary GJ and the new sprite began to radiate optical emissions at the trailing dead time of the forth frame. Therefore, only a part of the luminosity of the secondary GJ and the new sprite were

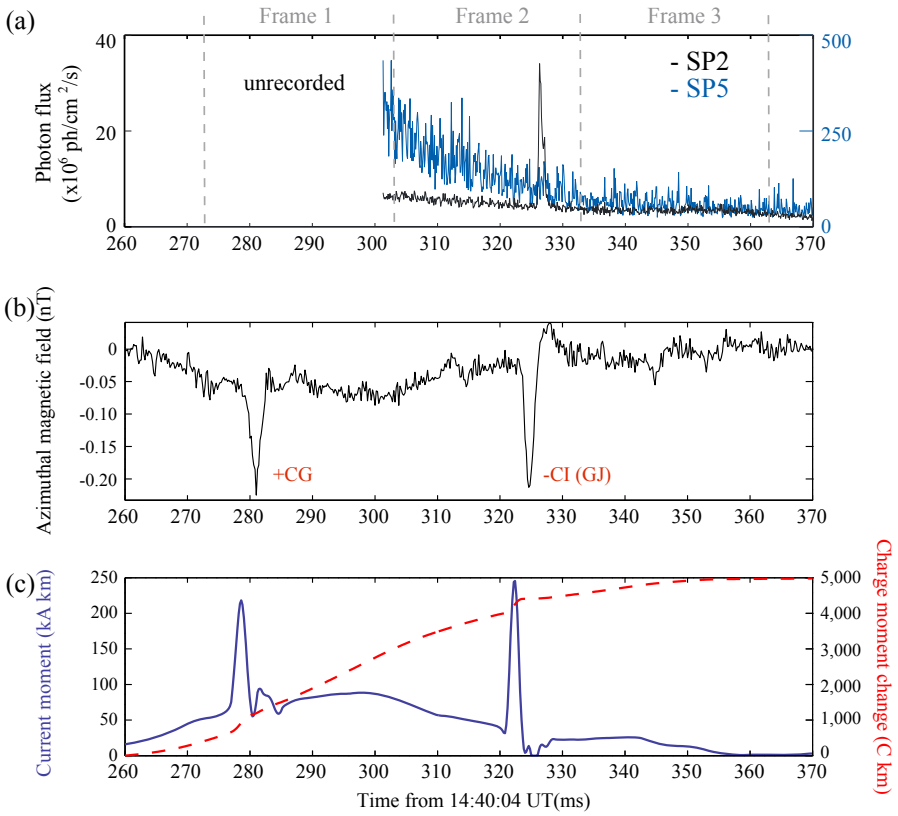

Figure 2. SP2 and SP5 data, the ULF azimuthal magnetic field waveform, and the source inferred current moment for event A. (a) The black and blue curves represent the SP2 and SP5 data, respectively. SP data of event A were not recorded before 14:40:04.302 UTC. (b) The ULF waveform contains two discernible pulses that are respectively associated with the sprite-inducing +CG and the GJ discharge (−CI) depicted in Figure 1. (c) The vertical current moment (blue curve) and the time-integrated charge moment change (red curve) are inferred from the ULF data shown in Figure 2b.

recorded in the fifth frame. However, except for the small gapping in the imagery data, characteristics of the optical, SP, and AP data are identical to those exhibited by events A and B.

3.2. Spectrophotometric Data

[9] The trigger time for event A is 14:40:04.326 UTC, and the temporal range of the SP data is from 14:40:04.301 UTC to 14:40:04.507 UTC. The operation setting of ISUAL at the times of recording these events was to save an extra image frame before the event trigger. Unfortunately, the trigger came in at the end of Frame 2. Thus, the SP only has data for the last 2 ms of Frame 1 and the spectral information of the preceding sprite and the sprite-inducing lightning were not recorded (see Figure 2a). The 0.1 ms time resolution data from the ISUAL SP (see Figure 1b) indicate that there are two sets of photometric peaks in the period of Frame 2 of Figure 1a. For the first set of peaks near 326.30 ms after 14:40:04.000 UTC, both SP2 and SP6 contain distinct photometric peaks, while the signals in SP1, SP3, and SP4 are only slightly above or buried in the background noise. Judging from the pronounced blue emissions [*Kuo et al.*, 2009; *Chou et al.*, 2010], it is asserted that this set of peaks is from the secondary GJ [*Lee et al.*, 2012]. For the second set of peaks near 327.10 ms, SP1, SP2, and SP4 show clearly identifiable peaks, while the photometric peaks in SP3 and SP6 are less distinct.

[10] The second set of peaks likely comes from the new sprite, due to its similarity to the spectra of follow-up sprites in the multi-sprite events (not shown). An additional support for this assertion can be obtained by computing the spectral ratio (SP2 versus SP4) for these TLEs. The SP2-to-SP4 ratio gives the relative intensity of the blue versus the red band emissions in a TLE. The ratios for events A, B, and C as well as those for multi-sprite events are tabulated in Table 1. The P1 and P2 in the table respectively denote the ratios for the preceding sprite and the follow-up sprite in multi-sprite sequences. The ISUAL SP5 (777.4 nm) emissions indicate that the follow-up sprites were induced by lightning strokes or by continuing current, and the images indicate that the sprites only share a small overlapping region (not shown here). For the multi-sprite events, the SP2-to-SP4 ratio for the preceding sprite is 0.26, while those for the follow-up sprites fall in the range of 0.15–0.17. For the presumed GJ-induced sprites (Table 1), the SP2-to-SP4 ratios for the second photometric peaks of events A, B, and C, respectively, are 0.15, 0.18, and 0.16, which are closer in value to those for the follow-up sprites than those for the preceding sprite in multi-sprite events. The reason why the GJ-induced sprites and the follow-up sprites have similar SP2-to-SP4 ratios could be that they have similar ambient environmental conditions. Both occur near and slightly overlap with the preceding sprites. Thus, the ambient environment may have been altered by the preceding sprites in a similar way.

Table 1. SP2/SP4 Ratios of GJ-Induced Sprites and Multi-sprite Events

Event Type	Event Date	SP2[a]	SP4[a]	SP2/SP4	SP2/SP4[b]	dT[c] (ms)
GJ-induced sprites	9 December 2009 (event A)	14.1	66.6	0.21	0.15	X
	3 August 2006 (event B)	15.8	62.6	0.25	0.18	X
	30 September 2008 (event C)	32.3	167.8	0.19	0.16	X
Sprites in multisprite events	7 August 2006 P1	69.8	221.4	0.32	0.26	
	7 August 2006 P2	6.1	33.0	0.18	0.15	~85
	26 November 2006 P2	3.4	19.3	0.18	0.15	~99
	17 June 2007 P2	31.9	126.3	0.25	0.17	~100

[a]In units of 10^6 photons/cm^2/s.
[b]The observation angle-dependent response of ISUAL SP channels has been corrected [*Kuo et al*., 2005].
[c]The time difference between the preceding and the follow-up sprites, which is determined from photometric data.

[11] Hence, the second set of peaks is most likely from the new sprite. The ISUAL SP5 data (Figures 1b and 2a) also show no pronounced peaks on top of the smoothly decaying signal in the interval of the second image frame. This means that there is no impulsive lightning stroke during this time, except for the cloud emissions contributed by the continuing current in the sprite-inducing +CG.

3.3. Altitude-Resolved Array Photometric Data

[12] The AP blue module channels (ch9–ch14; Figure 1c) covering the altitudinal ranges of the lightning, GJ, and the new sprite further support that there is no apparent impulsive emission from lightning in the interval of image Frame 2. The near-constant readings in AP ch9 imply that the diffusive, lingering cloud illumination in the second image frame likely has come from the continuing current of the preceding-sprite-inducing lightning that occurred in the first image frame. Also, a blue emission pulse appears to propagate upwards from ch9 to ch11, which have corresponding altitudes of 15 to 55 km during 326.2 to 326.45 ms. The occurring heights and the propagating nature of the pulse indicate that the GJ is the originator of this signal. However, the pulse profiles of ch12 and ch13 differ substantially from those in ch10 and ch11. Since the occurring altitudes of the GJ and the new sprite in image Frame 2 could both span the altitudes of 55 to 85 km, AP ch12 and ch13 apparently contain additional signal from the new sprites besides those from the GJ. The time of the peak optical emissions progressively increases from ch12 to ch14. This is a good indication that the luminous structure of the new sprite is also mainly upward developing.

[13] Based on the above analyses, it can be concluded that the first set of SP peaks and the upward propagating pulse in the AP blue module are from the secondary GJ, and ~1 ms after the occurrence of the GJ, a new sprite appears and produces the second set of SP peaks and the additional AP blue module signals in ch12 and ch13. Most importantly, there were no impulsive lightning emissions at the time of the new sprite, except for the decaying signal emitted by the continuing current in the preceding-sprite-inducing +CG. The time separation of the new sprite and the +CG lightning pulse that produced the clustering sprites is ~30–50 ms. Hence, the quasi-static E-field established in the upper atmosphere above the thundercloud by the +CG lightning pulse should have relaxed. This invokes an intriguing question: could the new sprites have been induced by the GJs? To assess this possibility, the electromagnetic characteristics of the secondary GJs have to be scrutinized closely. We will also examine the possibility of the new sprites being produced by the continuing current of the +CGs.

4. Radio Atmospheric Data

[14] Using the associated ULF data, we can infer the polarity, the vertical current moment, and the time-integrated CMC of the lightning and the GJ events. Of the three events studied in this work, only the magnetic ULF waveform (Figure 2b) for event A that has correct timing and bearing angle was found in the data recorded by the Lulin station. Unfortunately, the ULF signals for events B and C were missing because the Lulin station was down at both times. We emphasize that although in Figure 2 the luminous peak and the ULF peak for the secondary gigantic jet seem to misalign by ~2 ms, these two peaks are actually well aligned after correcting for the propagation delays from event A to the Lulin ULF antenna (~4100 km) and to the FORMOSAT-2 satellite (~3400 km) as well as the drift of the ISUAL clock.

[15] In Figure 2b, the pulse at 281.0 ms is believed to be emitted by the sprite-inducing +CG lightning, and the decaying signal following the pulse is from the continuing current. Meanwhile, the pulse at 325.0 ms was emitted by the current flowing in the discharge channel of the negative GJ (negative cloud-to-ionosphere discharge (−CI)). The peak current moment of the GJ is inferred as ~245 kA-km (Figure 2c). This value is much higher than those for the GJ events reported by *Cummer et al*. [2009] (55 kA-km) and *Huang et al*. [2012] (20–160 kA-km). With inferred current moments, the charge moment changes can be computed by integrating the current moment over a specific duration, and the CMC for event A is depicted in Figure 2c (red curve). The CMC of the clustering-sprite-inducing +CG is computed as ~600 C km for the first 5 ms, while the CMC for the first 4 ms is ~400 C km for the GJ. The CMC has accumulated to ~4000 C km before the −CI discharge occurs. However, it should be noted that there was an abnormal increase of magnetic field before the +CG pulse which might not have been radiated by the +CG discharge. The anomalous increase in B-field may be due to unknown atmospheric disturbances from unrelated lightning discharges. Therefore, the inferred CMC and current moment may have been overestimated.

5. The Probable Generating Mechanism and Discussions

[16] After analyzing the spectral and the associate electromagnetic data, the probable occurrence scenario of these complex events is proposed and illustrated in Figure 3. The removal of positive charge in the thundercloud by the +CG is equivalent to adding negative charge to the

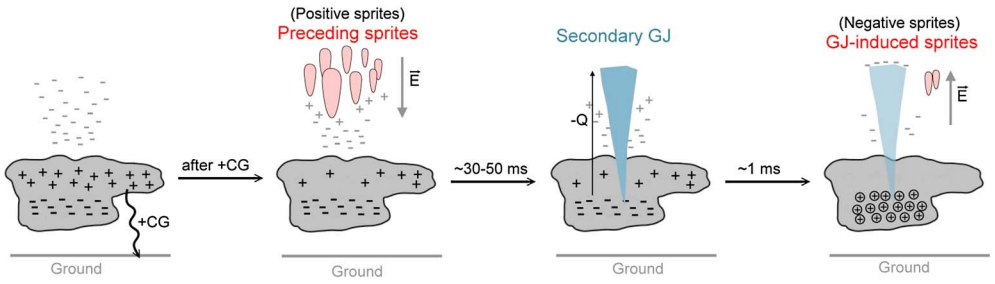

Figure 3. Probable generating scenario for the GJ-induced sprites. Red-shaded columns represent sprites, and the blue column represents the secondary GJ. Plus symbols denote the positive charges, minus symbols are for the negative charges, and plus symbols in a circle represent the electric holes. A simplified distribution of space charges above the thundercloud is also displayed. The time progresses from the left to the right and the time intervals are denoted above the arrows. A +CG produces a large and downward pointing quasi-electrostatic field above the thundercloud and induces the preceding sprites. About 30–50 ms later, a secondary GJ propagates upward and transfers a large amount of negative charge to the ionosphere which is equivalent to leaving electric holes in the cloud. The positive charges establish an upward quasi-electrostatic field which induces the new sprites.

thundercloud. Therefore, a large and downward pointing quasi-electrostatic field is created in the region above the thundercloud and induces the preceding sprites. However, at 60–90 km altitude, the quasi-electrostatic field due to the CG discharge pulse (not including the continuing current) cannot persist more than ~20 ms [*Pasko et al*., 1997] and should have decayed away before the occurrence of the GJ. About 30–50 ms after the occurrence of the preceding sprites, the secondary GJ transfers some of the negative charge in the cloud to the ionosphere and results in an upward pointing quasi-electrostatic field in the region above the thundercloud. The GJ-induced quasi-electrostatic field seems to be sufficiently large and impulsive to induce the sprites. In the scheme depicted above, the polarity of the negative GJ-induced sprites should be negative and should have a polarity opposite to those induced by +CGs.

[17] *Barrington-Leigh et al*. [1999] analyzed two −CG-induced sprites and reported that the −CG discharges had unusually large vertical charge moment changes of up to 1550 C km in 5 ms. *Li et al*. [2012] analyzed six negative sprites which were always accompanied by halos. They noted that the source current of the sprite parent lightning was very impulsive and produced CMC of at least 450 C km within 0.5 ms or less. Compared to positive-sprite-inducing lightning, the negative-sprite-inducing lightning is more impulsive and transfers a larger amount of charge in a shorter time. Therefore, these secondary GJs, those that have high current moments and accumulate large and over the threshold CMCs in a short time, appear to be capable of inducing negative sprites. However, if −CI discharges are indeed capable of inducing sprites, why do only these three secondary GJs initiate sprites while the stand-alone GJs do not?

[18] It may be that after the occurrence of the preceding sprites, the electron density in the volume occupied by the sprite is higher than that of the background. At these high altitudes, it takes several tens of milliseconds up to several seconds for the elevated density region to relax back to the ambient level [*Lehtinen and Inan*, 2007]. Under this circumstance, the upper channel of the secondary GJ develops through a preionized environment, a situation which is similar to the dart leaders propagating through the region previously ionized by the stepped leader. Hence, the propagation speeds of dart leaders are faster than those of stepped leaders [*Rakov and Uman*, 2003]. Therefore, the time needed for the secondary GJ to complete the channel, which links the cloud top and the lower ionosphere, could be shorter than that for the typical GJs. In addition, the preceding-sprite-inducing +CG, besides causing charge imbalance in the cloud, may have also depleted a large amount of upper positive charges. Hence, it may have produced a large potential difference between the upper positive charge and the midlevel negative charge layers, which leads to an unusually large amount of charge transferred by the secondary GJ to the lower ionosphere. To sum it up, the secondary GJ may have transferred a relatively large amount of charge in a shorter duration compared to the common GJs. This may explain why sprites could only be induced by secondary GJs but not by the typical GJs. This may also suggest that the rarity of GJ-induced sprites is due to the fact that secondary GJs are infrequent.

[19] However, the possibility of the new sprites being long-delayed sprites, which were induced by the continuing current associated with the preceding +CG, cannot be excluded. *Cummer and Füllekrug* [2001] analyzed three long-delayed sprites and concluded that for a +CG to initiate sprites with a delay time of 40 ms, the accumulated CMC needs to be ~2000 C km or greater. Based on a finite difference time domain model simulation, *Li et al*. [2008] reported that intense continuing current can enhance the mesospheric electric field and can further induce long-delayed sprites. *Li et al.* [2008, Figure 5] pointed out that a 40 ms-delayed-time sprite can be induced when the accumulated CMC exceeds ~1000 C km. From Figure 2c in this paper, the accumulated CMC from the onset of the lightning return stoke to the GJ initiation is ~3000 C km. Thus, for the sprites that occurred after the secondary GJs reported in this work, it is possible that the continuing current of the preceding +CGs may have been the inducers of the new sprites.

[20] However, it should further be noted that in *Cummer and Füllekrug* [2001, Figure 2] and *Li et al*. [2008, Figure 6], the current moment keeps increasing or remains constant before the sprite initiations, while the current moment of event A evidently was decaying before the new sprite initiated. A decaying current moment would be expected to be harder to initiate mesospheric breakdown. Moreover, *Li et al*. [2008] also pointed out that the initiation altitudes of the long-delayed sprites were slightly lower than those

of the short-delayed sprites. However, for event A, the altitude of the new sprite in Frame 2 of Figure 1a is similar to that of the preceding sprites in Frame 1. In addition, *Qin et al*. [2011] indicated that the upward propagating positive heads of negative sprite streamers should be brighter than the downward ones. The AP data of event A showed that the sprite emissions propagate upward, which is consistent with the new sprite being a negative sprite induced by the −CI GJ. The above mentioned features and considerations all favor the new sprites being induced by the secondary GJs.

[21] As a final note, for the three events reported here, regardless of the time separation between the new sprites and the preceding-sprite-inducing +CGs, the new sprites always appear near the secondary GJs and occur within ~1 ms relative to the GJs. This fact cannot be easily deemed as purely coincidental, though the mechanism of these complex events is still an open question and further numerical simulations clearly are needed to resolve this issue.

[22] **Acknowledgments.** Works were supported in part by the National Space Organization (NSPO) and National Science Council in Taiwan under grants NSPO-S-102005, NSC 99-2112-M-006-006-MY3, NSC 101-2119-M-006-011, NSC 101-2111-M-006-004, NSC 101-2119-M-006-009, NSC 100-2111-M-006-002, and NSC 101-2627-E-006-002.

[23] W. K. Peterson thanks Oscar van der Velde and an anonymous reviewer for their assistance in evaluating this paper.

References

Barrington-Leigh, C. P., U. S. Inan, M. Stanley, and S. A. Cummer (1999), Sprites triggered by negative lightning discharges, *Geophys. Res. Lett.*, *26*(24), 3605–3608, doi:10.1029/1999GL010692.

Chen, A. B., et al. (2008), Global distributions and occurrence rates of transient luminous events, *J. Geophys. Res.*, *113*, A08306, doi:10.1029/2008JA013101.

Chern, J. L., R. R. Hsu, H. T. Su, S. B. Mende, H. Fukunishi, Y. Takahashi, and L. C. Lee (2003), Global survey of upper atmospheric transient luminous events on the ROCSAT-2 satellite, *J. Atmos. Sol. Terr. Phys.*, *65*, 647–659, doi:10.1016/S1364-6826(02)00317-6.

Chou, J. K., et al. (2010), Gigantic jets with negative and positive polarity streamers, *J. Geophys. Res.*, *115*, A00E45, doi:10.1029/2009JA014831.

Cummer, S. A., and M. Füllekrug (2001), Unusually intense continuing current in lightning produces delayed mesospheric breakdown, *Geophys. Res. Lett.*, *28*(3), 495–498, doi:10.1029/2000GL012214.

Cummer, S. A. (2003), Current moment in sprite-producing lightning, *J. Atmos. Sol. Terr. Phys. 65*, 499–508, doi:10.1016/S1364-6826(02)00318-8.

Cummer, S. A., J. Li, F. Han, G. Lu, N. Jaugey, W. A. Lyons, and T. E. Nelson (2009), Quantification of the troposphere-to-ionosphere charge transfer in a gigantic jet, *Nat. Geosci.*, *2*, 617–620, doi:10.1038/ngeo607.

Huang, S.-M., C.-L. Hsu, A. B. Chen, J. Li, L.-J. Lee, G.-L. Yang, Y.-C. Wang, R.-R. Hsu, and H.-T. Su (2011), Effects of notch-filtering on the ELF sferics and the physical parameters, *Radio Sci.*, *46*, RS5014, doi:10.1029/2010RS004519.

Huang, S.-M., R.-R. Hsu, L.-J. Lee, H.-T. Su, C.-L. Kuo, C.-C. Wu, J.-K. Chou, S.-C. Chang, Y.-J. Wu, and A. B. Chen (2012), Optical and radio signatures of negative gigantic jets: Cases from Typhoon Lionrock (2010), *J. Geophys. Res.*, *117*, A08307, doi:10.1029/2012JA017600.

Krehbiel, P. R., J. A. Riousset, V. P. Pasko, R. J. Thomas, W. Rison, M. A. Stanley, and H. E. Edens (2008), Upward electrical discharges from thunderstorms, *Nat. Geosci.*, *1*, 233–237, doi:10.1038/ngeo162.

Kuo, C.-L., et al. (2005), Electric fields and electron energies inferred from the ISUAL recorded sprites, *Geophys. Res. Lett.*, *32*, 19103, doi:10.1029/2005GL023389.

Kuo, C.-L., et al. (2009), Discharge processes, electric field, and electron energy in ISUAL-recorded gigantic jets, *J. Geophys. Res.*, *114*, A04314, doi:10.1029/2008JA013791.

Lee, L.-J., et al. (2010), Controlling synoptic-scale factors for the distribution of transient luminous events, *J. Geophys. Res.*, *115*, A00E54, doi:10.1029/2009JA014823.

Lee, L.-J., S.-M. Huang, J.-K. Chou, C.-L. Kuo, A. B. Chen, H.-T. Su, R.-R. Hsu, H. U. Frey, Y. Takahashi, and L.-C. Lee (2012), Characteristics and generation of secondary jets and secondary gigantic jets, *J. Geophys. Res.*, *117*, A06317, doi:10.1029/2011JA017443.

Lehtinen, N. G., and U. S. Inan (2007), Possible persistent ionization caused by giant blue jets, *Geophys. Res. Lett.*, *34*, L08804, doi:10.1029/2006GL029051.

Li, J., S. A. Cummer, W. A. Lyons, and T. E. Nelson (2008), Coordinated analysis of delayed sprites with high-speed images and remote electromagnetic fields, *J. Geophys. Res.*, *113*, D20206, doi:10.1029/2008JD010008.

Li, J., S. Cummer, G. Lu, and L. Zigoneanu (2012), Charge moment change and lightning-driven electric fields associated with negative sprites and halos, *J. Geophys. Res.*, *117*, A09310, doi:10.1029/2012JA017731.

Lu, G., et al. (2011), Lightning development associated with two negative gigantic jets, *Geophys. Res. Lett.*, *38*, L12801, doi:10.1029/2011GL047662.

Marshall, R. A., and U. S. Inan (2007), Possible direct cloud-to-ionosphere current evidenced by sprite-initiated secondary TLEs, *Geophys. Res. Lett.*, *34*, L05806, doi:10.1029/2006GL028511.

Pasko, V. P., U. S. Inan, T. F. Bell, and Y. N. Taranenko (1997), Sprites produced by quasi-electrostatic heating and ionization in the lower ionosphere, *J. Geophys. Res.*, *102*(A3), 4529–4561, doi:10.1029/96JA03528.

Pasko, V. P., M. A. Stanley, J. D. Mathews, U. S. Inan, and T. G. Wood (2002), Electrical discharge from a thundercloud top to the lower ionosphere, *Nature*, *416*, 152–154, doi:10.1038/416152a.

Qin, J., S. Celestin, and V. P. Pasko (2011), On the inception of streamers from sprite halo events produced by lightning discharges with positive and negative polarity, *J. Geophys. Res.*, *116*, A06305, doi:10.1029/2010JA016366.

Rakov, V. A., and M. A. Uman (2003), Lightning: Physics and Effects, 687 pp., Cambridge Univ. Press, New York.

Sentman, D. D., E. M. Wescott, D. L. Osborne, D. L. Hampton, and M. J. Heavner (1995), Preliminary results from the Sprites94 aircraft campaign: 1. Red sprites, *Geophys. Res. Lett.*, *22*, 1205–1208, doi:10.1029/95GL00583.

Su, H. T., R. R. Hsu, A. B. Chen, Y. C. Wang, W. S. Hsiao, W. C. Lai, L. C. Lee, M. Sato, and H. Fukunishi (2003), Gigantic jets between a thundercloud and the ionosphere, *Nature*, *423*, 974–976, doi:10.1038/ nature01759.

Taylor, M. J., et al. (2008), Rare measurements of a sprite with halo event driven by a negative lightning discharge over Argentina, *Geophys. Res. Lett.*, *35*, L14812, doi:10.1029/2008GL033984.

van der Velde, O. A., W. A. Lyons, T. E. Nelson, S. A. Cummer, J. Li, and J. Bunnell (2007), Analysis of the first gigantic jet recorded over continental North America, *J. Geophys. Res.*, *112*, D20104, doi:10.1029/2007JD008575.

van der Velde, O. A., J. Bór, J. Li, S. A. Cummer, E. Arnone, F. Zanotti, M. Füllekrug, C. Haldoupis, S. NaitAmor, and T. Farges (2010), Multi-instrumental observations of a positive gigantic jet produced by a winter thunderstorm in Europe, *J. Geophys. Res.*, *115*, D24301, doi:10.1029/2010JD014442.